Determining the strong phase of the a_1 meson decay amplitude using the $W \to \nu\tau(\to\nu a_1(\to\pi^\mp\pi^\mp\pi^\pm))$ process

Kaoru Hagiwara,[1] Hiroyuki Ishida,[1] Toshifumi Yamada,[2] and Daneng Yang[3]

[1]KEK Theory Center, Tsukuba, Ibaraki 305-0801, Japan
[2]Institute of Science and Engineering, Shimane University, Matsue 690-8504, Japan
[3]Department of Physics, Tsinghua University, Beijing 100084, China

(Received 7 January 2020; accepted 3 February 2020; published 19 February 2020)

To measure the helicity of a spin-1 meson from the triple vector product of the three-momenta of its decay products, one needs information about the strong phase of the decay amplitude. In this paper, taking $a_1(1260)$ meson as an example, we present a method to extract information about the strong phase from the triple vector product of the pion momenta in the $W \to \nu\tau(\to\nu a_1(\to\pi^\mp\pi^\mp\pi^\pm))$ process, where the a_1 helicity is known *a priori* from electroweak theory. This process is advantageous in that highly boosted a_1^- mesons from τ_L^- decays have nearly maximal helicity asymmetry and thus most reflect the strong phase. We revisit the theoretical calculation of the a_1 meson helicity in the $W \to \nu\tau(\to\nu a_1)$ process. Next, we formulate the differential decay rate of polarized a_1 mesons in a manner convenient for the study of the a_1 meson helicity asymmetry. Finally, we present the method for extracting information about the strong phase, and assess its feasibility at the LHC.

DOI: 10.1103/PhysRevD.101.034023

I. INTRODUCTION

The helicity of spin-1 mesons can be a probe for physics beyond the Standard Model (SM). For example, in the $B^- \to K^-\pi^-\pi^+\gamma$ process induced by $b \to s\gamma$, the SM predicts that the $K^-\pi^-\pi^+$ system is mostly left-handed because the W boson loop gives an amplitude with a left-handed photon, while various extensions of the SM contain an extra amplitude with a right-handed photon. The helicity of the $K^-\pi^-\pi^+$ system can be determined from the triple vector product of the three-momenta of K^-, π^-, π^+, and indeed a nonzero polarization of the system has been confirmed experimentally [1]. Nevertheless, the helicity has not been measured. The difficulty lies in the fact that the triple vector product of three-momenta is a naïve T-odd quantity [2] (odd under the reversal of all three-momenta and spins), and in CP-conserving theories like QCD its expectation value is nonzero only with the strong phase of the decay amplitude of $K^-\pi^-\pi^+$ resonances, which is poorly understood. Since $K_1(1270)$ and $K_1(1400)$ resonances (the latter is much suppressed) contribute to the $B^- \to K^-\pi^-\pi^+\gamma$ process [3], efforts have been made to theoretically or phenomenologically determine the strong phase of $K_1(1270)$ and $K_1(1400)$ decay amplitudes [4–9]. Notably, Ref. [8] has pursued a purely phenomenological approach where one extracts, from experimental data on the $B^- \to K^-\pi^-\pi^+J/\psi$ process, information about the strong phase necessary for the $K_1(1270)$ helicity measurement.

In this paper, we study experimental determination of the strong phase of a spin-1 meson's decay amplitude which utilizes a hadronic decay of a τ lepton from a W boson decay. Since the helicity of a spin-1 meson in the decay of a polarized τ is known *a priori* from electroweak theory, we can use $W \to \nu\tau(\to\nu A)$ events (A denotes a spin-1 meson) to determine the strong phase. Moreover, the $W \to \nu\tau(\to\nu A)$ process is advantageous in that highly boosted spin-1 mesons in $W \to \nu\tau(\to\nu A)$ events have nearly maximal helicity asymmetry (i.e. almost purely left-handed or right-handed) and hence the impact of the strong phase is maximized. Although our ultimate target is the strong phase of $K_1(1270)$ and $K_1(1400)$ decay amplitudes, in this paper we deal with a simpler case with an $a_1(1260)$ meson. We present a method to phenomenologically determine the strong phase of the $a_1^- \to \pi^-\pi^-\pi^+$ decay amplitude[1,2] from $W \to \nu\tau(\to\nu a_1(\to\pi^\mp\pi^\mp\pi^\pm))$ data (Fig. 1), and assess its feasibility in W boson production events at the LHC.

Once the strong phase of the $a_1^- \to \pi^-\pi^-\pi^+$ decay amplitude is determined, one can use it to search for new physics through the a_1 polarization. Moreover, we expect that the strong phase of the $K_1^- \to K^-\pi^-\pi^+$ decay

[1]Throughout the paper, a_1 refers to $a_1(1260)$ meson.
[2]Theoretical study on the hadronic form factors of $a_1^- \to \pi^-\pi^-\pi^+$ decay amplitude is found, e.g., in Refs. [10–12].

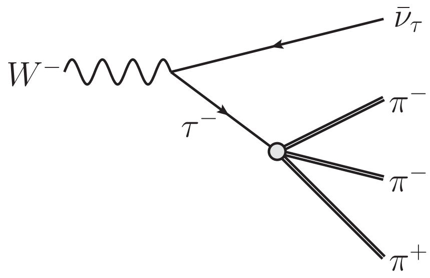

FIG. 1. $W \to \nu\tau(\to \nu a_1(\to \pi^\mp\pi^\mp\pi^\pm))$ process.

amplitude is determined in basically the same manner, which is then utilized for the most interesting case, the photon polarization measurement in the $B^- \to K^-\pi^-\pi^+\gamma$ process.

This paper is organized as follows:

In Sec. II, we revisit the theoretical calculation of the helicity of a_1^- meson in the $W^- \to \bar{\nu}_\tau\tau^-(\to\nu_\tau a_1^-)$ process. The a_1^- helicity is calculated as a function of the energy fraction of a_1^- in τ^- decay in the laboratory frame, $z = E_{a_1}/E_\tau$. We will confirm that a_1^- with $z \gtrsim 0.8$ (i.e. highly boosted a_1^-) is almost purely left-handed.

In Sec. III, we express the differential decay rate of polarized a_1^- mesons using the following parametrization: Let p_1, p_2, p_3 respectively denote the four-momenta of π^-, π^-, π^+, with $Q \cdot p_1 > Q \cdot p_2$ ($Q = p_1 + p_2 + p_3$). In an a_1^- rest frame, we write the angle between $\vec{p}_3 \times \vec{p}_1$ and a_1^-'s boost direction in the laboratory frame as Ψ, and write the angle between $\vec{p}_3$ and the projection of a_1^-'s boost direction onto the a_1^- decay plane as ϕ. The angles Ψ, ϕ and the Dalitz variables $s_{13} = (p_1 + p_3)^2$, $s_{23} = (p_2 + p_3)^2$ completely parametrize the differential decay rate. A benefit of this parametrization is that that part of the differential decay rate which reflects the a_1^- helicity asymmetry is simply linear in $\cos\Psi$ and is independent of ϕ.[3]

In Sec. IV, we present a method to determine the strong phase using $W \to \nu\tau(\to\nu a_1(\to\pi^\mp\pi^\mp\pi^\pm))$ events, based on the theoretical calculation of the a_1^- helicity in Sec. II and the parametrization of the differential decay rate in Sec. III. Statistical uncertainty in the above determination at the 14 TeV LHC with 300 fb^{-1} of data is further estimated.

Section V summarizes the paper.

In the Appendix, we give a simple derivation of the Wigner rotation, which is used in the calculation of the a_1^- helicity in boosted τ^- decays in Sec. II.

II. a_1^- HELICITY IN THE $W^- \to \bar{\nu}_\tau\tau^-(\to\nu_\tau a_1^-)$ PROCESS

Since τ^- in the $W^- \to \tau^-\bar{\nu}_\tau$ process is almost purely left-handed, it suffices to consider polarized τ^-. The differential decay rate of the $\tau^- \to \nu_\tau\pi^-\pi^-\pi^+$ process with polarized τ^- is expressed as

$$\begin{aligned} &\mathrm{d}\Gamma(\tau_h^- \to \pi^-\pi^-\pi^+\nu_\tau) \\ &\quad = \frac{1}{2m_\tau}\left|\sum\nolimits_{\lambda=\pm,0}\mathcal{M}(\tau_h^- \to \nu_\tau a_{1,\lambda}^-)B_{a_1}(Q^2)\mathcal{M}(a_{1,\lambda}^- \to \pi^-\pi^-\pi^+)\right|^2 \mathrm{d}\Phi_2(\tau \to a_1\nu)\frac{\mathrm{d}Q^2}{2\pi}\mathrm{d}\Phi_3(a_1 \to 3\pi), \\ &h = \pm\frac{1}{2}: \tau^- \text{ helicity}, \qquad \lambda = \pm, 0: a_1^- \text{ helicity}, \qquad Q^\mu: a_1^- \text{ momentum}. \end{aligned} \tag{1}$$

$\mathcal{M}(\tau_h^- \to \nu_\tau a_{1,\lambda}^-)$ denotes the helicity amplitude of the $\tau^- \to \nu_\tau a_1^-$ process, $B_{a_1}(Q^2)$ is the form factor of a_1 resonance that satisfies $B(Q^2 = 0) = 1$, and $\mathcal{M}(a_{1,\lambda}^- \to \pi^-\pi^-\pi^+)$ denotes the helicity amplitude of the $a_1^- \to \pi^-\pi^-\pi^+$ process. $\mathrm{d}\Phi_2(\tau \to a_1\nu)$ and $\mathrm{d}\Phi_3(a_1 \to 3\pi)$ denote the phase space factors of $\tau^- \to \nu_\tau a_1^-$ and $a_1^- \to \pi^-\pi^-\pi^+$ processes, respectively. In Eq. (1), the contribution from $\pi(1300)$ resonance is neglected, since the OPAL Collaboration has reported, based on a fitting of $\tau^- \to \pi^-\pi^-\pi^+\nu$ data, that the branching ratio of $\tau^- \to \pi^-(1300)\nu$ process is below 0.84% of the total $\tau^- \to \pi^-\pi^-\pi^+\nu$ branching ratio [14]. Also, a single axial-vector resonance, $a_1(1260)$, is assumed to dominate the process, since the CLEO Collaboration has reported that the same assumption yields a good fit to the isospin-related process $\tau^- \to \pi^-\pi^0\pi^0\nu$ [15]. Note that the vector current contribution is negligible in the $\tau^- \to \pi^-\pi^-\pi^+\nu_\tau$ process due to G-parity of QCD.

Integrating out the azimuthal angle of a_1^- momentum around the τ^- helicity axis, we remove interference among amplitudes with different a_1^- helicities. The differential decay rate is then factorized into the one for the $\tau^- \to \nu_\tau a_1^-$ process and the one for the $a_1^- \to \pi^-\pi^-\pi^+$ process, and is expressed as

$$\begin{aligned} &\mathrm{d}\Gamma(\tau_h^- \to \nu_\tau\pi^-\pi^-\pi^+) \\ &\quad = \frac{1}{2m_\tau}\sum_{\lambda=\pm1,0}|\mathcal{M}(\tau_h^- \to \nu_\tau a_{1,\lambda}^-)|^2|B_{a_1}(Q^2)|^2 \\ &\quad \times |\mathcal{M}(a_{1,\lambda}^- \to \pi^-\pi^-\pi^+)|^2 \\ &\quad \times \frac{1}{16\pi}\left(1 - \frac{Q^2}{m_\tau^2}\right)\mathrm{d}\cos\hat{\theta}\frac{\mathrm{d}Q^2}{2\pi}\mathrm{d}\Phi_3(a_1 \to 3\pi) \end{aligned} \tag{2}$$

[3] Kühn-Mirkes parametrization [13] has been widely used for describing the $\tau^- \to 3\pi\nu_\tau$ decay kinematics. Our parametrization differs from it in that the coordinate is defined independently of τ^- momentum, namely, purely the $a_1^- \to 3\pi$ decay kinematics is described.

where $\hat{\theta}$ denotes the angle between the a_1^- momentum and the τ^- helicity axis in a τ^- rest frame. For convenience, we trade $\hat{\theta}$ for the energy fraction of a_1^- in τ^- decay in the laboratory frame, z,

$$z = \frac{E_{a_1}}{E_\tau} = \frac{1 + Q^2/m_\tau^2 + \beta(1 - Q^2/m_\tau^2)\cos\hat{\theta}}{2} \tag{3}$$

where β denotes the speed of τ^- in the laboratory frame. Equation (2) is then rewritten as

$$\begin{aligned} &\mathrm{d}\Gamma(\tau_h^- \to \nu_\tau \pi^-\pi^-\pi^+) \\ &\quad = |B_{a_1}(Q^2)|^2 2\sqrt{Q^2}\frac{\mathrm{d}Q^2}{2\pi} \\ &\quad\times \sum_{\lambda=\pm1,0} \frac{\mathrm{d}\Gamma(\tau_h^- \to \nu_\tau a_{1,\lambda}^-)}{\mathrm{d}z}\mathrm{d}z\mathrm{d}\Gamma(a_{1,\lambda}^- \to \pi^-\pi^-\pi^+), \end{aligned} \tag{4}$$

with

$$\frac{\mathrm{d}\Gamma(\tau_h^- \to \nu_\tau a_{1,\lambda}^-)}{\mathrm{d}z} = \frac{1}{\beta}\frac{1}{16\pi m_\tau}|\mathcal{M}(\tau_h^- \to \nu_\tau a_{1,\lambda}^-)|^2, \tag{5}$$

$$\begin{aligned} \mathrm{d}\Gamma(a_{1,\lambda}^- \to \pi^-\pi^-\pi^+) &= \frac{1}{2\sqrt{Q^2}}|\mathcal{M}(a_{1,\lambda}^- \to \pi^-\pi^-\pi^+)|^2 \\ &\quad\times \mathrm{d}\Phi_3(a_1 \to 3\pi). \end{aligned} \tag{6}$$

$\mathrm{d}\Gamma(\tau_h^- \to \nu_\tau a_{1,\lambda}^-)/\mathrm{d}z$ corresponds to the differential decay rate of τ^- with helicity h decaying into a_1^- with helicity λ, for a specific value of z. $\mathrm{d}\Gamma(a_{1,\lambda}^- \to \pi^-\pi^-\pi^+)$ corresponds to the differential decay rate of a_1^- with helicity λ. $\mathrm{d}\Gamma(\tau_h^- \to \nu_\tau a_{1,\lambda}^-)/\mathrm{d}z$ for $h = -1/2$ encodes the a_1^- helicity distribution in the $W^- \to \bar{\nu}_\tau \tau^-(\to \nu_\tau a_1^-)$ process.

In the rest of the section, we evaluate $\mathrm{d}\Gamma(\tau_h^- \to \nu_\tau a_{1,\lambda}^-)/\mathrm{d}z$. The helicity amplitude $\mathcal{M}(\tau_h^- \to \nu_\tau a_{1,\lambda}^-)$ is given by

$$\begin{aligned} &\mathcal{M}(\tau_h^- \to \nu_\tau a_{1,\lambda}^-) \\ &\quad = \sqrt{2}G_F\cos\theta_C\,\bar{\nu}_\tau\gamma^\mu\frac{1-\gamma_5}{2}\tau(\vec{p}_\tau, h)\epsilon_\mu^*(Q^2,\lambda), \end{aligned} \tag{7}$$

where we retain Q^2 dependence of the polarization vector ϵ_μ, since a_1 is a broad resonance. The helicity amplitude $\mathcal{M}(\tau_h^- \to \nu_\tau a_{1,\lambda}^-)$ is specified in terms of the a_1^- helicity along the a_1^- boost direction in a τ^- rest frame, λ_τ, and the angle between the a_1^- momentum and the τ^- helicity axis in a τ^- rest frame $\hat{\theta}$; we find

$$\mathcal{M}(\tau_h^- \to \nu_\tau a_{1,\lambda_\tau}^-) = \sqrt{2}G_F\cos\theta_C\sqrt{m_\tau^2 - Q^2}\hat{\mathcal{M}}_{h\lambda_\tau}, \tag{8}$$

where

$$\hat{\mathcal{M}}_{-\frac{1}{2},-} = \sqrt{2}\cos\frac{\hat{\theta}}{2},\quad \hat{\mathcal{M}}_{-\frac{1}{2},0} = \frac{m_\tau}{\sqrt{Q^2}}\sin\frac{\hat{\theta}}{2},\quad \hat{\mathcal{M}}_{-\frac{1}{2},+} = 0, \tag{9}$$

$$\hat{\mathcal{M}}_{\frac{1}{2},-} = -\sqrt{2}\sin\frac{\hat{\theta}}{2},\quad \hat{\mathcal{M}}_{\frac{1}{2},0} = \frac{m_\tau}{\sqrt{Q^2}}\cos\frac{\hat{\theta}}{2},\quad \hat{\mathcal{M}}_{\frac{1}{2},+} = 0. \tag{10}$$

Experimentally, what we measure is the a_1^- helicity along the a_1^- boost direction in the laboratory frame, λ_{lab}, not the helicity along the a_1^- boost direction in a τ^- rest frame λ_τ. Hence, we want to rewrite Eq. (8) in terms of λ_{lab}. For this purpose, we expand the a_1^- polarization vectors in the laboratory frame in terms of those in a τ rest frame, as

$$\begin{aligned} \epsilon^\mu(Q^2,\lambda_{\mathrm{lab}}) &= \sum_{\lambda_\tau=\pm1,0}\{-\epsilon^\mu(Q^2,\lambda_\tau)\epsilon^{\nu*}(Q^2,\lambda_\tau)\}\epsilon_\nu(Q^2,\lambda_{\mathrm{lab}}) \\ &= \sum_{\lambda_\tau=\pm1,0}\{-\epsilon^{\nu*}(Q^2,\lambda_\tau)\epsilon_\nu(Q^2,\lambda_{\mathrm{lab}})\}\epsilon^\mu(Q^2,\lambda_\tau) \\ &= \sum_{\lambda_\tau=\pm1,0} d^{J=1}_{\lambda_\tau\lambda_{\mathrm{lab}}}(\tilde{\theta})\epsilon^\mu(Q^2,\lambda_\tau), \end{aligned} \tag{11}$$

where $d^{J=1}_{\lambda'\lambda}$ is a d-function, and $\tilde{\theta}$ is the angle between the a_1^- boost direction in a τ^- rest frame and that in the laboratory frame, measured in an a_1^- rest frame. $\tilde{\theta}$ is expressed in terms of the angle between the a_1^- momentum and the τ^- helicity axis in a τ^- rest frame $\hat{\theta}$, and the speed and boost factor of τ^- in the laboratory frame β and $\gamma = 1/\sqrt{1-\beta^2}$, as (see the Appendix for the derivation)

$$\begin{aligned} \cos\tilde{\theta} &= \frac{(1+a^2)\beta\cos\hat{\theta} + 1 - a^2}{\sqrt{\{(1+a^2)+(1-a^2)\beta\cos\hat{\theta}\}^2 - 4a^2/\gamma^2}} \\ &\quad (a = \sqrt{Q^2}/m_\tau), \end{aligned} \tag{12}$$

or equivalently, in terms of the energy fraction of a_1^- in τ^- decay in the laboratory frame z, as

$$\cos\tilde{\theta} = \frac{z(1+a^2) - 2a^2}{(1-a^2)\sqrt{z^2 - \frac{a^2}{\gamma^2}}} \qquad (z = E_{a_1}/E_\tau). \tag{13}$$

The helicity amplitude is rewritten in terms of the a_1^- helicity in the laboratory frame λ_{lab}, as

$$\mathcal{M}(\tau_h^- \to \nu_\tau a_{1,\lambda_{\mathrm{lab}}}^-) = \sum_{\lambda_\tau=\pm1,0} d^{J=1}_{\lambda_\tau\lambda_{\mathrm{lab}}}(\tilde{\theta})\hat{\mathcal{M}}_{h\lambda_\tau}(\hat{\theta}) \tag{14}$$

with $\tilde{\theta}$ given in Eq. (12) or Eq. (13).

Assembling Eqs. (5), (8), (14), (13), we numerically calculate $\mathrm{d}\Gamma(\tau_h^- \to \nu_\tau a_{1,\lambda}^-)/\mathrm{d}z$ and present it in the form of the normalized differential decay rate

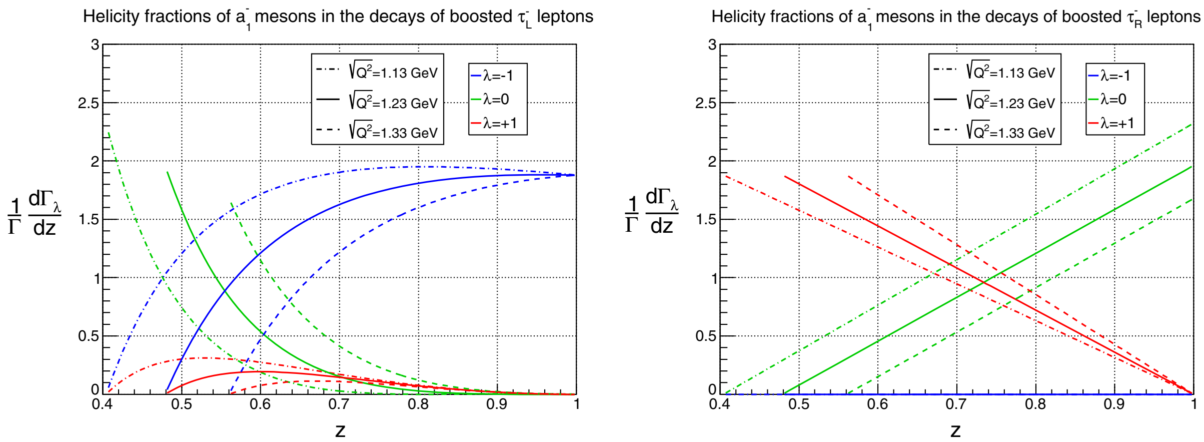

FIG. 2. Left: normalized differential decay rate Eq. (15) for τ^- with helicity $h = -1/2(\tau_L^-)$, for each final-state a_1^- helicity in the laboratory frame $\lambda_{\rm lab} = \pm, 0$. The horizontal axis is $z = E_{a_1}/E_\tau$, the energy fraction of a_1^- in τ^- decay in the laboratory frame. The boost factor of τ^- in the laboratory frame is fixed as $\gamma = 23$. The dot-dashed, solid, and dashed lines correspond to different a_1^- invariant masses $\sqrt{Q^2} = 1.13$ GeV, 1.23 GeV, 1.33 GeV. Right: same as the left plot except that τ^- has helicity $h = 1/2(\tau_R^-)$.

$$\frac{1}{\Gamma}\frac{{\rm d}\Gamma_{\lambda_{\rm lab}}}{{\rm d}z}(z, Q^2) = \frac{1}{\sum_{\lambda=\pm1,0}\int {\rm d}z' \frac{{\rm d}\Gamma(\tau_h^-\to\nu_\tau a_{1,\lambda}^-;z',Q^2)}{{\rm d}z'}}\frac{{\rm d}\Gamma(\tau_h^- \to \nu_\tau a_{1,\lambda_{\rm lab}}^-; z, Q^2)}{{\rm d}z} \tag{15}$$

in Fig. 2, for each τ^- helicity $h = -1/2$ (τ_L^-) and $h = 1/2$ (τ_R^-). The boost factor of τ^- is fixed as $\gamma = 23$, corresponding to the boost factor of τ^- from the decay of a W boson at rest. However, the plots are almost independent of γ when $\gamma \gtrsim 3$. Three different values of the a_1^- invariant mass, $\sqrt{Q^2} = 1.13$ GeV, 1.23 GeV, 1.33 GeV, are considered.

The left panel of Fig. 2 presents the a_1^- helicity in the $W^- \to \bar{\nu}_\tau \tau^-(\to \nu_\tau a_1^-)$ process. In the left panel, we observe that the a_1^- meson with $z \gtrsim 0.8$ is almost purely left-handed ($\lambda_{\rm lab} = -1$).

We note that Fig. 2 is in agreement with the preceding study Ref. [16].

III. DIFFERENTIAL DECAY RATE OF POLARIZED a_1^- MESONS

We formulate the differential decay rate of the $a_1^- \to \pi^-\pi^-\pi^+$ process for each a_1^- helicity, Eq. (6), in a manner convenient for the study of the helicity asymmetry.

The helicity amplitude is written as

$$\mathcal{M}(a_{1,\lambda}^- \to \pi^-\pi^-\pi^+) = \epsilon^\mu(Q^2, \lambda) J_\mu, \tag{16}$$

where $\epsilon^\mu(Q, \lambda)$ is the polarization vector of a_1^- with helicity λ, and J_μ is the hadronic current,

$$J^\mu = \langle \pi^-\pi^-\pi^+ | (-\bar{u}\gamma^\mu\gamma^5 d) | 0 \rangle. \tag{17}$$

The most general parametrization for the hadronic current J^μ that respects (i) Lorentz covariance, (ii) the current conservation $Q^\mu J_\mu = 0$, and (iii) Bose symmetry of two π^-'s, is given as follows: Let p_1, p_2, p_3 respectively denote the momenta of π^-, π^-, π^+ [then $Q^\mu = (p_1 + p_2 + p_3)^\mu$], where the two π^-'s are distinguished by $Q \cdot p_1 > Q \cdot p_2$. The most general parametrization is then

$$J^\mu(p_1, p_2, p_3) = -i\frac{2\sqrt{2}}{3f_\pi}\{(p_{1\nu} - p_{3\nu})F(Q^2, s_{13}, s_{23}) + (p_{2\nu} - p_{3\nu})F(Q^2, s_{23}, s_{13})\}\left(g^{\mu\nu} - \frac{Q^\mu Q^\nu}{Q^2}\right), \tag{18}$$

where $s_{13} \equiv (p_1 + p_3)^2$ and $s_{23} \equiv (p_2 + p_3)^2$, $f_\pi \simeq 93$ MeV is the pion decay constant, and $F(Q^2, s_{13}, s_{23})$ is a general function of three Lorentz scalars. $F(Q^2, s_{13}, s_{23})$ is normalized in such a way that if $\pi\pi$ resonances were absent, we would have $F(Q^2, s_{13}, s_{23}) = 1$ by chiral perturbation theory [17].

We explicitly write the a_1^- decay helicity amplitude Eq. (16) in the a_1^- rest frame whose z-axis is along the a_1^- boost direction in the laboratory frame (thus $\lambda_{\rm lab}$ is along this z-axis). In this frame, the momenta of the three pions and their sum can be parametrized as

$$Q^\mu = (\sqrt{Q^2}, 0, 0, 0), \tag{19}$$

$$p_3^\mu = (E_3, \vec{p}_3) = \frac{1}{2\sqrt{Q^2}}\begin{pmatrix} x_3 \\ \tilde{x}_3 \cos\phi \cos\Psi \\ \tilde{x}_3 \sin\phi \\ -\tilde{x}_3 \sin\Psi \cos\phi \end{pmatrix}, \tag{20}$$

$$p_1^\mu = (E_1, \vec{p}_1) = \frac{1}{2\sqrt{Q^2}} \begin{pmatrix} x_1 \\ \tilde{x}_1 \cos\Psi(\cos\phi\cos\theta_1 - \sin\phi\sin\theta_1) \\ \tilde{x}_1(\sin\phi\cos\theta_1 + \cos\phi\sin\theta_1) \\ -\tilde{x}_1\sin\Psi(\cos\phi\cos\theta_1 - \sin\phi\sin\theta_1) \end{pmatrix}, \tag{21}$$

$$p_2^\mu = (E_2, \vec{p}_2) = \frac{1}{2\sqrt{Q^2}} \begin{pmatrix} x_2 \\ \tilde{x}_2 \cos\Psi(\cos\phi\cos\theta_2 + \sin\phi\sin\theta_2) \\ \tilde{x}_2(\sin\phi\cos\theta_2 - \cos\phi\sin\theta_2) \\ -\tilde{x}_2\sin\Psi(\cos\phi\cos\theta_2 + \sin\phi\sin\theta_2) \end{pmatrix}, \tag{22}$$

where x_i and $\tilde{x}_i$ are defined in terms of Q^2, s_{13}, s_{23} as

$$x_i = 2Q\cdot p_i = Q^2 - s_{jk} + m_\pi^2 \quad ((i,j,k) = (1,2,3),(2,3,1),(3,1,2)), \tag{23}$$

$$\tilde{x}_i = \sqrt{x_i^2 - 4Q^2 m_\pi^2}. \tag{24}$$

θ_i ($i = 1, 2$) denotes the angle between $\vec{p}_i$ and $\vec{p}_3$, which is given in terms of $\tilde{x}_i$ as

$$\cos\theta_1 = \frac{\tilde{x}_2^2 - \tilde{x}_1^2 - \tilde{x}_3^2}{2\tilde{x}_1\tilde{x}_3}, \qquad \cos\theta_2 = \frac{\tilde{x}_1^2 - \tilde{x}_2^2 - \tilde{x}_3^2}{2\tilde{x}_2\tilde{x}_3}. \tag{25}$$

Ψ is the angle between the $\vec{p}_3 \times \vec{p}_1$ vector and the z-axis, and ϕ is the angle between the $\vec{p}_3$ vector and the projection of the z-axis onto the a_1^- decay plane, which satisfy

$$\vec{p}_3 \times \vec{p}_1 = \frac{1}{4Q^2}\tilde{x}_3\tilde{x}_1 \sin\theta_1(\sin\Psi, 0, \cos\Psi). \tag{26}$$

The polarization vectors are given by

$$\epsilon^\mu(Q^2, \lambda_{\rm lab} = \pm) = \frac{1}{\sqrt{2}}(0, \mp 1, -i, 0), \quad \epsilon^\mu(Q^2, \lambda_{\rm lab} = 0) = (0,0,0,1). \tag{27}$$

From Eqs. (16), (18), (27), the helicity amplitudes are expressed as

$$\mathcal{M}(a^-_{1,\lambda_{\rm lab}=\pm} \to \pi^-\pi^-\pi^+) = \frac{1}{3f_\pi}\frac{1}{\sqrt{Q^2}}[\pm\cos\Psi\{\cos\phi A(Q^2, s_{13}, s_{23}) - \sin\phi B(Q^2, s_{13}, s_{23})\} + i\{\sin\phi\, A(Q^2, s_{13}, s_{23}) + \cos\phi\, B(Q^2, s_{13}, s_{23})\}], \tag{28}$$

$$\mathcal{M}(a^-_{1,\lambda_{\rm lab}=0} \to \pi^-\pi^-\pi^+) = \frac{\sqrt{2}}{3f_\pi}\frac{1}{\sqrt{Q^2}}\sin\Psi\{\cos\phi\, A(Q^2, s_{13}, s_{23}) - \sin\phi\, B(Q^2, s_{13}, s_{23})\}, \tag{29}$$

where A and B are structure functions with mass dimension +2 defined as[4] [remember that $\tilde{x}_i$ is related to Q^2, s_{13}, s_{23} through Eq. (24)]

$$A(Q^2, s_{13}, s_{23}) = (\cos\theta_1\tilde{x}_1 - \tilde{x}_3)F(Q^2, s_{13}, s_{23}) + (\cos\theta_2\tilde{x}_2 - \tilde{x}_3)F(Q^2, s_{23}, s_{13}), \tag{32}$$

$$B(Q^2, s_{13}, s_{23}) = \sin\theta_1\tilde{x}_1\{F(Q^2, s_{13}, s_{23}) - F(Q^2, s_{23}, s_{13})\}. \tag{33}$$

[4]In the $m_\pi \to 0$ limit, they asymptote as

$$A(Q^2, s_{13}, s_{23}) \overset{m_\pi\to 0}{\longrightarrow} \left(x_1 - x_3 - \frac{2(1-x_2)}{x_3}\right)F(Q^2, s_{13}, s_{23}) + \left(x_2 - x_3 - \frac{2(1-x_1)}{x_3}\right)F(Q^2, s_{23}, s_{13}), \tag{30}$$

$$B(Q^2, s_{13}, s_{23}) \overset{m_\pi\to 0}{\longrightarrow} \frac{2}{x_3}\sqrt{(1-x_1)(1-x_2)(1-x_3)}\{F(Q^2, s_{13}, s_{23}) - F(Q^2, s_{23}, s_{13})\}. \tag{31}$$

Finally, we plug Eqs. (28), (29) into the formula for the polarized a_1^- differential decay rate

$$\mathrm{d}\Gamma(a^-_{1,\lambda_{\mathrm{lab}}} \to \pi^-\pi^-\pi^+) = \frac{1}{2\sqrt{Q^2}}|\mathcal{M}(a^-_{1,\lambda_{\mathrm{lab}}} \to \pi^-\pi^-\pi^+)|^2 \mathrm{d}\Phi_3(a_1 \to 3\pi)$$
$$= \frac{1}{2\sqrt{Q^2}}|\mathcal{M}(a^-_{1,\lambda_{\mathrm{lab}}} \to \pi^-\pi^-\pi^+)|^2 \frac{1}{128\pi^3}\frac{1}{Q^2}\mathrm{d}s_{13}\mathrm{d}s_{23}\frac{\mathrm{d}\cos\Psi}{2}\frac{\mathrm{d}\phi}{2\pi}$$

and obtain

$$\frac{\mathrm{d}^4\Gamma(a^-_{1,\lambda_{\mathrm{lab}}=\pm} \to \pi^-\pi^-\pi^+)}{\mathrm{d}\cos\Psi \mathrm{d}\phi \mathrm{d}s_{13}\mathrm{d}s_{23}} = \frac{1}{512\pi^4}\frac{1}{2Q^4\sqrt{Q^2}}\frac{1}{9f_\pi^2}[|A|^2+|B|^2-(1-\cos^2\Psi)\{\cos^2\phi|A|^2+\sin^2\phi|B|^2-\sin 2\phi \mathrm{Re}(A\cdot B^*)\} \pm 2\cos\Psi\,\mathrm{Im}(A\cdot B^*)], \tag{34}$$

$$\frac{\mathrm{d}^4\Gamma(a^-_{1,\lambda_{\mathrm{lab}}=0} \to \pi^-\pi^-\pi^+)}{\mathrm{d}\cos\Psi \mathrm{d}\phi \mathrm{d}s_{13}\mathrm{d}s_{23}} = \frac{1}{512\pi^4}\frac{1}{2Q^4\sqrt{Q^2}}\frac{1}{9f_\pi^2}2(1-\cos^2\Psi)\{\cos^2\phi|A|^2+\sin^2\phi|B|^2-\sin 2\phi\,\mathrm{Re}(A\cdot B^*)\}. \tag{35}$$

Consider a general a_1 production process, not limited to the $W \to \nu\tau(\to a_1\nu)$ process. In terms of the transverse and asymmetric helicity fractions in the laboratory frame defined by

$$P_T = \frac{(\text{Number of } a_1^- \text{ mesons with } \lambda_{\mathrm{lab}} = +) + (\text{Number of } a_1^- \text{ mesons with } \lambda_{\mathrm{lab}} = -)}{(\text{Total number of } a_1^- \text{ mesons})},$$
$$P_A = \frac{(\text{Number of } a_1^- \text{ mesons with } \lambda_{\mathrm{lab}} = +) - (\text{Number of } a_1^- \text{ mesons with } \lambda_{\mathrm{lab}} = -)}{(\text{Total number of } a_1^- \text{ mesons})},$$

the a_1^- differential decay rate in a general a_1 production process satisfies

$$\frac{1}{\Gamma(a_1^- \to \pi^-\pi^-\pi^+)}\frac{\mathrm{d}^4\Gamma(a_1^- \to \pi^-\pi^-\pi^+)}{\mathrm{d}\cos\Psi \mathrm{d}\phi \mathrm{d}s_{13}\mathrm{d}s_{23}}$$
$$= P_T\frac{1}{4\pi N_{\mathrm{nor}}}[|A|^2+|B|^2-3(1-\cos^2\Psi)\{\cos^2\phi|A|^2+\sin^2\phi|B|^2-\sin 2\phi\,\mathrm{Re}(A\cdot B^*)\}] \tag{36}$$

$$+ P_A\frac{1}{4\pi N_{\mathrm{nor}}}2\cos\Psi\,\mathrm{Im}(A\cdot B^*) \tag{37}$$

$$+ \frac{1}{4\pi N_{\mathrm{nor}}}2(1-\cos^2\Psi)\{\cos^2\phi|A|^2+\sin^2\phi|B|^2-\sin 2\phi\,\mathrm{Re}(A\cdot B^*)\}, \tag{38}$$

where

$$N_{\mathrm{nor}} = \frac{2}{3}\iint \mathrm{d}s_{12}\mathrm{d}s_{13}(|A|^2+|B|^2).$$

From Eq. (37), we find that the $\cos\Psi$ asymmetry is proportional to both the helicity asymmetry P_A and the term $\mathrm{Im}(A\cdot B^*)/N_{\mathrm{nor}}$, the latter of which is nonzero only with the strong phase. $\cos\Psi$ is a naïve T-odd quantity, and its expectation value is nonzero only with the strong phase, in accordance with what is stated in Sec. I.

Once the function $\mathrm{Im}(A\cdot B^*)/N_{\mathrm{nor}}$ is known, one can measure P_A using asymmetry of the number of events with $\cos\Psi > 0$ and $\cos\Psi < 0$. Conversely, if the helicity asymmetry of a_1^- is known *a priori*, one can determine $\mathrm{Im}(A\cdot B^*)/N_{\mathrm{nor}}$ by measuring the asymmetry of the number of events with $\cos\Psi > 0$ and $\cos\Psi < 0$. This is indeed feasible in the $\tau_L^- \to \nu_\tau a_1^-(\to\pi^-\pi^-\pi^+)$ process, for which the a_1^- helicity is theoretically calculable as done in Sec. II. To be specific, we write the differential decay rate of the $\tau_L^- \to \nu_\tau a_1^-(\to\pi^-\pi^-\pi^+)$ process in terms of $\frac{1}{\Gamma}\frac{\mathrm{d}\Gamma_{\lambda_{\mathrm{lab}}}}{\mathrm{d}z}$ Eq. (15) for τ_L^- as

$$\frac{1}{\Gamma(\tau_L^- \to \nu_\tau a_1^-(\to\pi^-\pi^-\pi^+))}\frac{d^5\Gamma(\tau_L^- \to \nu_\tau a_1^-(\to\pi^-\pi^-\pi^+))}{d\cos\Psi d\phi ds_{13}ds_{23}dz}$$
$$= \left(\frac{1}{\Gamma}\frac{d\Gamma_+}{dz}+\frac{1}{\Gamma}\frac{d\Gamma_-}{dz}\right)\frac{1}{4\pi N_{\rm nor}}[|A|^2+|B|^2-(1-\cos^2\Psi)$$
$$\times\{\cos^2\phi|A|^2+\sin^2\phi|B|^2-\sin 2\phi\,{\rm Re}(A\cdot B^*)\}] \quad (39)$$

$$+\left(\frac{1}{\Gamma}\frac{d\Gamma_+}{dz}-\frac{1}{\Gamma}\frac{d\Gamma_-}{dz}\right)\frac{1}{4\pi N_{\rm nor}}2\cos\Psi\,{\rm Im}(A\cdot B^*) \quad (40)$$

$$+\frac{1}{\Gamma}\frac{d\Gamma_0}{dz}\frac{1}{4\pi N_{\rm nor}}2(1-\cos^2\Psi)\{\cos^2\phi|A|^2$$
$$+\sin^2\phi|B|^2-\sin 2\phi\,{\rm Re}(A\cdot B^*)\}. \quad (41)$$

Since $\frac{1}{\Gamma}\frac{d\Gamma_{\lambda_{\rm lab}}}{dz}$ can be computed theoretically, it is possible to determine ${\rm Im}(A\cdot B^*)/N_{\rm nor}$ from the $\cos\Psi$ asymmetry of $\tau_L^- \to \nu_\tau a_1^-(\to\pi^-\pi^-\pi^+)$ events. A problem is that when we use $pp\to W^\mp \to \nu\tau^\mp(\to\nu\pi^\mp\pi^\mp\pi^\pm)$ events to collect τ_L^-, it is difficult to reconstruct z, since two neutrinos contribute to the missing transverse momentum. In this paper, we evade the reconstruction of z by exploiting a positive correlation between z and a_1^-'s transverse mass M_T. We impose a tight selection cut on M_T and thereby select events with large z. ${\rm Im}(A\cdot B^*)/N_{\rm nor}$ is determined from the $\cos\Psi$ asymmetry of events, divided by the convolution of theoretically calculated $\frac{1}{\Gamma}\frac{d\Gamma_+}{dz}-\frac{1}{\Gamma}\frac{d\Gamma_-}{dz}$ and the reweighting function of z under given selection cuts (the reweighting function is obtainable from a Monte Carlo simulation).

An advantage of the above method is that, for τ_L^- and for large z, $|\frac{1}{\Gamma}\frac{d\Gamma_+}{dz}-\frac{1}{\Gamma}\frac{d\Gamma_-}{dz}|$ is maximized (see the left panel of Fig. 2). Hence, the $\cos\Psi$ asymmetry is maximized and the statistical uncertainty in the determination of ${\rm Im}(A\cdot B^*)/N_{\rm nor}$ is reduced.

We comment that, for τ_L^- and for $z\to 1$, $\frac{1}{\Gamma}\frac{d\Gamma_+}{dz}-\frac{1}{\Gamma}\frac{d\Gamma_-}{dz}$ quickly approaches to its value at $z=1$ and is insensitive to the precise value of z. Hence, once we collect large-z events, the convolution of $\frac{1}{\Gamma}\frac{d\Gamma_+}{dz}-\frac{1}{\Gamma}\frac{d\Gamma_-}{dz}$ and the reweighting function of z is not affected by details of the reweighting function, which reduces the systematic uncertainty associated with the estimation of the reweighting function. However, confirming this reduction of the systematic uncertainty is beyond the scope of the present paper.

IV. METHOD TO DETERMINE ${\rm Im}(A\cdot B^*)/N_{\rm nor}$

A. Method

${\rm Im}(A\cdot B^*)/N_{\rm nor}$ satisfies the following relation stemming from Eq. (40):

$$\frac{{\rm Im}(A\cdot B^*)}{N_{\rm nor}}(Q^2,s_{13},s_{23})N(Q^2)\left(\frac{1}{\Gamma}\frac{d\Gamma_+}{dz}-\frac{1}{\Gamma}\frac{d\Gamma_-}{dz}\Big|_{z,Q^2,\text{for }\tau_L^-}\right)$$
$$=\frac{d^3N}{dzds_{13}ds_{23}}(\cos\Psi>0;z,Q^2,s_{13},s_{23})$$
$$-\frac{d^3N}{dzds_{13}ds_{23}}(\cos\Psi<0;z,Q^2,s_{13},s_{23}) \quad (42)$$

where $d^3N(\cos\Psi>0;z,Q^2,s_{13},s_{23})/dzds_{13}ds_{23}$ denotes the number of $pp\to W^\mp\to\nu\tau^\mp(\to\nu\pi^\mp\pi^\mp\pi^\pm)$ events with $\cos\Psi>0$ per z,s_{13},s_{23} for fixed Q^2 (and likewise for $\cos\Psi<0$), and $N(Q^2)$ is the total number of events for any z,s_{13},s_{23} for fixed Q^2 given by

$$N(Q^2)$$
$$=\int dz\iint ds_{12}ds_{13}\left\{\frac{d^3N}{dzds_{13}ds_{23}}(\cos\Psi>0;z,Q^2,s_{13},s_{23})\right.$$
$$\left.+\frac{d^3N}{dzds_{13}ds_{23}}(\cos\Psi<0;z,Q^2,s_{13},s_{23})\right\}. \quad (43)$$

Remember that $N(Q^2)$ and ${\rm Im}(A\cdot B^*)/N_{\rm nor}$ do not depend on z.

In real experiments, we cannot measure the right-hand side of Eq. (42), since we do not reconstruct z. Instead, we propose to measure the following quantity:

$$\frac{d^2N_{\rm cut}}{ds_{13}ds_{23}}(\cos\Psi>0;Q^2,s_{13},s_{23})$$
$$-\frac{d^2N_{\rm cut}}{ds_{13}ds_{23}}(\cos\Psi<0;Q^2,s_{13},s_{23}), \quad (44)$$

where $d^2N_{\rm cut}(\cos\Psi>0;Q^2,s_{13},s_{23})/ds_{13}ds_{23}$ denotes the number of events with $\cos\Psi>0$ per s_{13}, s_{23} for fixed Q^2, *under given selection cuts* on the absolute values of the transverse momentum and pseudorapidity of a_1, the absolute value of the missing transverse momentum, and a_1's transverse mass. When one flips the sign of all three-momentum vectors, the above selection cuts are invariant and so are z,Q^2,s_{13},s_{23} and ϕ. On the other hand, $\cos\Psi$, which is proportional to the triple vector product of $\vec{p}_3,\vec{p}_1$ and the a_1 boost direction, flips its sign. As a result, if z,Q^2,s_{13},s_{23},ϕ are the same, the above selection cuts do not discriminate an event with $\cos\Psi=c$ and one with $\cos\Psi=-c$. Therefore, we can recast Eq. (44) in the form

$$(44)=\int dz\,f_{\rm cut}(z,Q^2,s_{13},s_{23})$$
$$\times\left\{\frac{d^3N}{dzds_{13}ds_{23}}(\cos\Psi>0;z,Q^2,s_{13},s_{23})\right.$$
$$\left.-\frac{d^3N}{dzds_{13}ds_{23}}(\cos\Psi<0;z,Q^2,s_{13},s_{23})\right\} \quad (45)$$

where $f_{\rm cut}(z, Q^2, s_{13}, s_{23})$ denotes the fraction of events with specific values of z, Q^2, s_{13}, s_{23} that pass the selection cuts, which is common for $\cos\Psi > 0$ and $\cos\Psi < 0$. From Eqs. (42), (45) and z-independence of $N(Q^2)$ and $\mathrm{Im}(A\cdot B^*)/N_{\rm nor}$, we have

$$\frac{\mathrm{Im}(A\cdot B^*)}{N_{\rm nor}}(Q^2, s_{13}, s_{23})N(Q^2)\int \mathrm{d}z\, f_{\rm cut}(z, Q^2, s_{13}, s_{23})\left(\frac{1}{\Gamma}\frac{\mathrm{d}\Gamma_+}{\mathrm{d}z} - \frac{1}{\Gamma}\frac{\mathrm{d}\Gamma_-}{\mathrm{d}z}\bigg|_{z,Q^2,\text{for }\tau_L^-}\right)$$
$$= \frac{\mathrm{d}^2N_{\rm cut}}{\mathrm{d}s_{13}\mathrm{d}s_{23}}(\cos\Psi > 0; Q^2, s_{13}, s_{23}) - \frac{\mathrm{d}^2N_{\rm cut}}{\mathrm{d}s_{13}\mathrm{d}s_{23}}(\cos\Psi < 0; Q^2, s_{13}, s_{23}). \quad (46)$$

The right-hand side is measured in experiments. As for the left-hand side, $N(Q^2)$ is known from the $pp \to W^\mp$ total cross section and branching fractions of $W^- \to \tau^-\bar{\nu}_\tau$ and $\tau^- \to \pi^-\pi^-\pi^+\nu_\tau$ decays. $\frac{1}{\Gamma}\frac{\mathrm{d}\Gamma_{\lambda_{\rm lab}}}{\mathrm{d}z}$ has been calculated theoretically in Sec. II. $f_{\rm cut}(z, Q^2, s_{13}, s_{23})$ can be evaluated with a Monte Carlo simulation by exploiting generator-level information on z. Therefore, it is possible to determine $\mathrm{Im}(A\cdot B^*)/N_{\rm nor}$.

For practical purposes, it is convenient to use $w(z, Q^2, s_{13}, s_{23})$ defined below, in place of $f_{\rm cut}(z, Q^2, s_{13}, s_{23})$:

$$w(z, Q^2, s_{13}, s_{23}) = \frac{N(Q^2) f_{\rm cut}(z, Q^2, s_{13}, s_{23})}{N_{\rm cut}(Q^2)} \quad (47)$$

where $N_{\rm cut}(Q^2)$ is the total number of events for fixed Q^2 that pass the selection cuts,

$$N_{\rm cut}(Q^2) = \iint \mathrm{d}s_{12}\mathrm{d}s_{13}\left\{\frac{\mathrm{d}^2N_{\rm cut}}{\mathrm{d}s_{13}\mathrm{d}s_{23}}(\cos\Psi > 0; Q^2, s_{13}, s_{23}) + \frac{\mathrm{d}^2N_{\rm cut}}{\mathrm{d}s_{13}\mathrm{d}s_{23}}(\cos\Psi < 0; Q^2, s_{13}, s_{23})\right\}. \quad (48)$$

$w(z, Q^2, s_{13}, s_{23})$ is interpreted as the reweighting of events with specific values of z, s_{13}, s_{23}, Q^2 due to the selection cuts, which is again common for $\cos\Psi > 0$ and $\cos\Psi < 0$. In terms of $w(z, Q^2, s_{13}, s_{23})$, Eq. (46) is recast in the form

$$\frac{\mathrm{Im}(A\cdot B^*)}{N_{\rm nor}}(Q^2, s_{13}, s_{23})N_{\rm cut}(Q^2)\int \mathrm{d}z\, w(z, Q^2, s_{13}, s_{23})\left(\frac{1}{\Gamma}\frac{\mathrm{d}\Gamma_+}{\mathrm{d}z} - \frac{1}{\Gamma}\frac{\mathrm{d}\Gamma_-}{\mathrm{d}z}\bigg|_{z,Q^2,\text{for }\tau_L^-}\right)$$
$$= \frac{\mathrm{d}^2N_{\rm cut}}{\mathrm{d}s_{13}\mathrm{d}s_{23}}(\cos\Psi > 0; Q^2, s_{13}, s_{23}) - \frac{\mathrm{d}^2N_{\rm cut}}{\mathrm{d}s_{13}\mathrm{d}s_{23}}(\cos\Psi < 0; Q^2, s_{13}, s_{23}). \quad (49)$$

In Sec. IV B, we generate detector-level Monte Carlo events for the 14 TeV LHC and impose selection cuts on them. Using these events, in Sec. IV C, we evaluate $w(z, Q^2, s_{13}, s_{23})$. In Sec. IV D, we estimate statistical uncertainty in a measurement of the right-hand side of Eq. (49) with 300 fb^{-1} of data.

B. Monte Carlo event generation and selection cuts

Using MadGraph5_aMC@NLO [18] with the TauDecay package [19], we generate parton-level events for the process (charged-conjugated process is also considered),

$$pp \to W^-(\to\bar{\nu}_\tau\tau^-(\to\nu_\tau\pi^-\pi^-\pi^+)) + 0,1,2\ \text{parton(s)} \quad (50)$$

for $\sqrt{s} = 14$ TeV pp collisions. Then, we use PYTHIA8 [20] to simulate parton showering. The groups of events with 0, 1, 2 parton(s) are matched with MLM-matching [21] algorithm.

For the events generated, we use the Delphes3 program [22] to simulate the CMS detector effects, considering $|\eta_{\tau\text{-jet}}| < 2.5$, $p_{\tau\text{-jet}T} > 1$ GeV and 60% tagging efficiency for the identification of a three-prong τ-jet. We reconstruct an a_1^- meson from a three-prong τ-jet by requiring that the three charged tracks have charges summed to that of a_1^- and that the invariant mass (calculated by assuming that each charged track is a pion) be less than 2 GeV. The variables $\cos\Psi$, s_{13}, s_{23} are calculated as described in Sec. III.

We impose the following selection cuts on the above samples:

(i) Event must contain exactly one reconstructed a_1^- meson.
(ii) Missing transverse momentum must satisfy $\not{p}_T > 25$ GeV.
(iii) Invariant mass of the a_1^- must satisfy $1.26\ \text{GeV} > \sqrt{Q^2} > 1.20$ GeV.

Additionally, we impose

(i) Transverse mass for the a_1^-,

$$M_T = \sqrt{2|\vec{\not{p}}_T|\sqrt{|\vec{p}_{a_1 T}|^2 + Q^2}(1-\cos\phi_{a_1\not{p}_T})} \quad (51)$$

where $\vec{p}_{a_1 T}$ denotes the transverse momentum of the a_1^-, and $\phi_{a_1\not{p}_T}$ is the azimuthal angle between the a_1^- and the missing transverse momentum, must satisfy either $M_T > 50$, 60, or 70 GeV.

The number of the sum of W^+ and W^- events with 300 fb^{-1} of data at each stage of event selection and for each M_T cut is tabulated in Table I.

C. Estimation of $w(z, Q^2, s_{13}, s_{23})$

Using the above event samples, we estimate $w(z, Q^2, s_{13}, s_{23})$ Eq. (47), which is the reweighting of events with specific values of z, s_{13}, s_{23}, Q^2 due to the selection cuts, which is common for $\cos\Psi > 0$ and $\cos\Psi < 0$. In fact, the selection cuts of Sec. IV B do not distort the distributions of Q^2, s_{13}, s_{23} and we simply have

$$w(z,Q^2,s_{13},s_{23}) = w(z) \quad \text{for } 1.26\,\text{GeV} > \sqrt{Q^2} > 1.20\,\text{GeV},$$
$$w(z,Q^2,s_{13},s_{23}) = 0, \qquad \text{otherwise}.$$

In Fig. 3, we present $w(z)$ for the selection cuts with $M_T > 50$, 60, and 70 GeV and for the case without M_T cut. We have confirmed that large-z events are efficiently collected with a tight M_T cut such as $M_T > 70$ GeV.

D. Statistical uncertainty

We estimate statistical uncertainty in a measurement of the right hand side of Eq. (49) with 300 fb^{-1} of data.

The statistical uncertainty is given as follows: Let δN_+ (δN_-) denote the number of events after the selection cuts of Sec. IV B, in a bin of Q^2, s_{13}, s_{23} with $\cos\Psi > 0$ ($\cos\Psi < 0$). If the bins are sufficiently narrow, the right-hand side of Eq. (49) is approximated by

TABLE I. Number of the sum of $pp \to W^\mp \to \nu\tau^\mp(\to \nu\pi^\mp\pi^\mp\pi^\pm)$ events at the 14 TeV LHC with 300 fb^{-1} of data, after each selection cut.

Selection cut	Number of W^+ and W^- events
One reconstructed a_1^- and $\not{p}_T > 25$ GeV	40.7×10^6
& 1.26 GeV > $\sqrt{Q^2}$ > 1.20 GeV	5.12×10^6
& $M_T > 50$ GeV	4.47×10^6
& $M_T > 60$ GeV	3.00×10^6
& $M_T > 70$ GeV	1.43×10^6

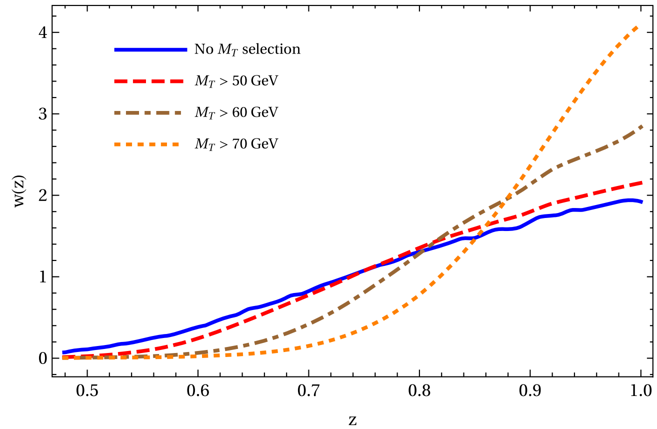

FIG. 3. $w(z)$, the reweighting of events with specific value of z due to the selection cuts of Sec. IV B (which does not depend on s_{13}, s_{23} and is uniform in the bin of Q^2). The cases with $M_T > 50$, 60, and 70 GeV and the case without M_T cut are plotted.

$$\delta N_+ - \delta N_-, \quad (52)$$

for which the ratio of the statistical uncertainty over its value is given by

$$\frac{\Delta_{\mathrm{stat}}(\delta N_+ - \delta N_-)}{\delta N_+ - \delta N_-} = \frac{\sqrt{\delta N_+ + \delta N_-}}{\delta N_+ - \delta N_-}. \quad (53)$$

This corresponds to the relative statistical uncertainty in the determination of $\mathrm{Im}(A\cdot B^*)/N_{\mathrm{nor}}$, and hence we obtain

$$\frac{\Delta_{\mathrm{stat}}(\mathrm{Im}(A\cdot B^*)/N_{\mathrm{nor}})}{\mathrm{Im}(A\cdot B^*)/N_{\mathrm{nor}}} = \frac{\sqrt{\delta N_+ + \delta N_-}}{\delta N_+ - \delta N_-}. \quad (54)$$

In Fig. 4, we present the relative statistical uncertainty Eq. (54) in each bin of (s_{13}, s_{23}) with 1.26 GeV > $\sqrt{Q^2}$ > 1.20 GeV, for various M_T cuts, at the 14 TeV LHC with 300 fb^{-1} of data.

We observe that the relative statistical uncertainty is below 2% in multiple bins of (s_{13}, s_{23}), and so the determination of $\mathrm{Im}(A\cdot B^*)/N_{\mathrm{nor}})$ is feasible at the 14 TeV LHC with 300 fb^{-1} of data, at least in light of statistics.

A tighter M_T cut diminishes overall statistics, but it enhances the relative $\cos\Psi$ asymmetry $|\frac{\delta N_+ - \delta N_-}{\delta N_+ + \delta N_-}|$, because this asymmetry is proportional to $|\frac{1}{\Gamma}\frac{d\Gamma_+}{dz} - \frac{1}{\Gamma}\frac{d\Gamma_-}{dz}|$ and the latter is largest for $z \sim 1$. Nevertheless, we do not find improvement in relative statistical uncertainty with tighter M_T cuts. This is because in the present simulation, the loss of overall statistics is more significant than the enhancement of the relative $\cos\Psi$ asymmetry.

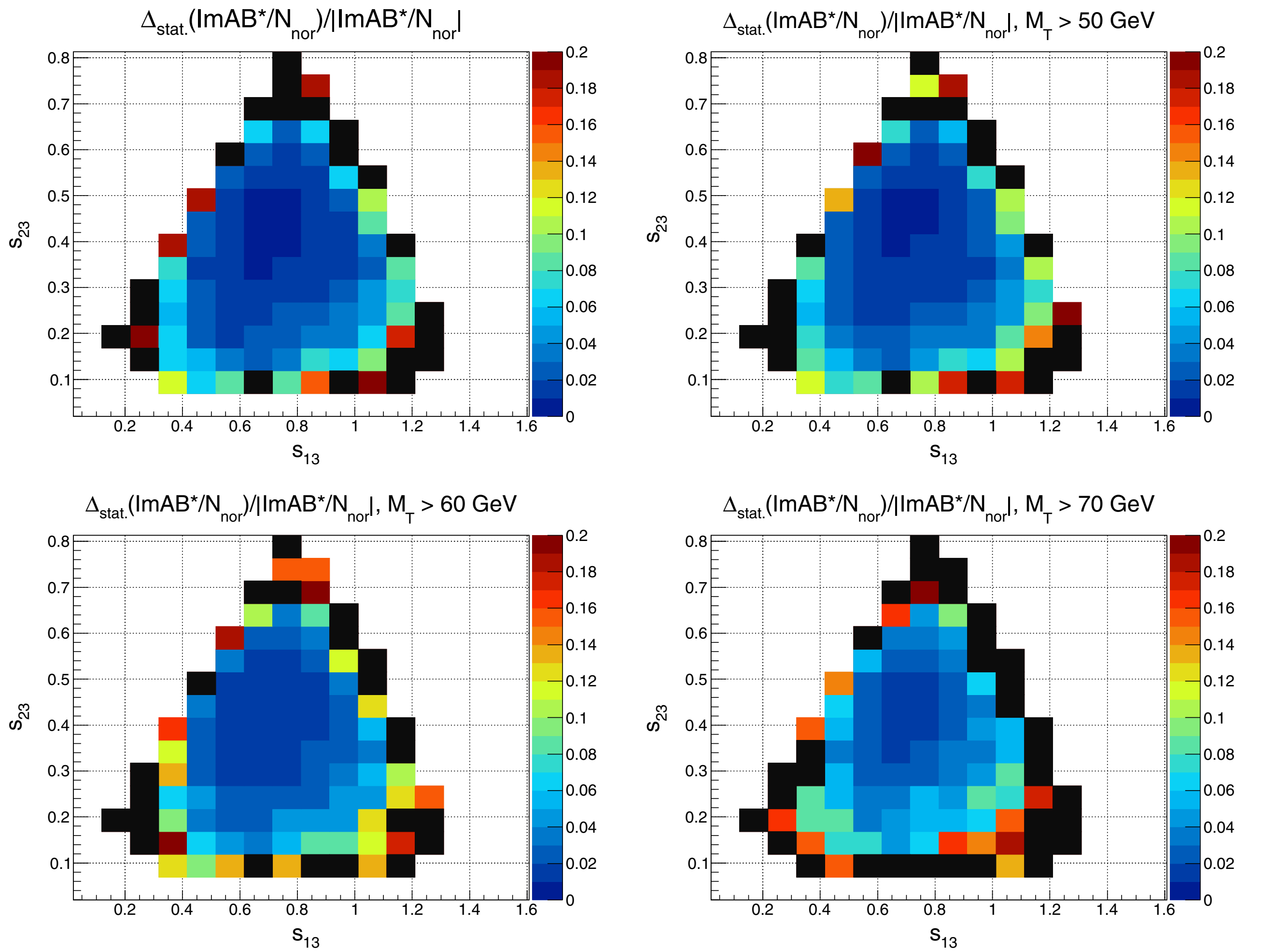

FIG. 4. Relative statistical uncertainty in the determination of $\mathrm{Im}(A\cdot B^*)/N_{\mathrm{nor}}$ at the 14 TeV LHC with 300 fb^{-1} of data, in each bin of (s_{13}, s_{23}) (in units of GeV^2) with 1.26 GeV $> \sqrt{Q^2} >$ 1.20 GeV. The upper-left, upper-right, lower-left, and lower-right panels correspond to the event selection without M_T cut, with $M_T > 50$ GeV, with $M_T > 60$ GeV, and with $M_T > 70$ GeV, respectively.

V. SUMMARY

We have presented a method to extract information about the strong phase of the $a_1^- \to \pi^-\pi^-\pi^+$ decay amplitude necessary for the a_1 helicity measurement. Our method utilizes $W \to \nu\tau(\to\nu\pi^\mp\pi^\mp\pi^\pm)$ events, for which the a_1 helicity is theoretically calculable. The method has an advantage that a_1^- mesons from τ_L^- decays with large boost (i.e. with $z = E_{a_1}/E_\tau \sim 1$ in the laboratory frame) have nearly maximal helicity asymmetry and thus most reflect the strong phase. We have revisited the theoretical calculation of the a_1^- helicity in the laboratory frame in the $W^- \to \bar{\nu}_\tau\tau^-(\to\nu_\tau a_1^-)$ process. We have formulated the differential decay rate of polarized a_1 mesons, where the information about the strong phase necessary for the helicity measurement is encapsulated by the term $\mathrm{Im}(A\cdot B^*)/N_{\mathrm{nor}}$. Finally, we have proposed a method to determine $\mathrm{Im}(A\cdot B^*)/N_{\mathrm{nor}}$ from $pp \to W \to \nu\tau(\to\nu\pi^\mp\pi^\mp\pi^\pm)$ events, and by estimating the statistical uncertainty at the 14 TeV LHC with 300 fb^{-1} of data, we have revealed that this method is feasible at least in the light of statistics.

ACKNOWLEDGMENTS

K. H. thanks Bernd Kniehl and members of II. Institut für Theoretische Physik, Universität Hamburg, where part of the work was done. K. H. and T. Y. thank Korea Institute for Advanced Study, where part of the work was done. D. Y. thanks the KEK Theory Center for the warm hospitality, and Qiang Li for continuous support. The numerical simulations were performed on the Computing Cluster at the Center of High Energy Physics, Tsinghua University. This work is partially supported by Scientific Grants by the Ministry of Education, Culture, Sports, Science and Technology of Japan, No. 19K147101 (T. Y.) and No. 18H03708 (H. I.).

APPENDIX: WIGNER ROTATION

The rotation between two angular momentum quantization axes of a massive particle in its rest frame, where the

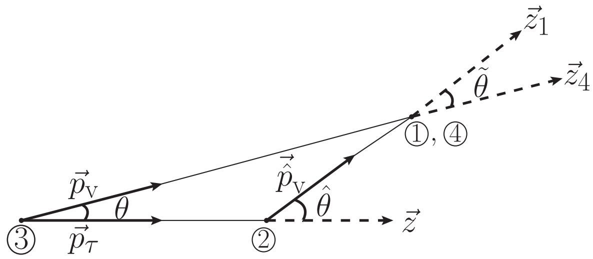

FIG. 5. Wigner rotation angle $\tilde{\theta}$. ① and ④ are vector meson rest frames, where $\vec{z}_1$ is chosen along the meson momentum direction in the τ rest frame ②, whereas $\vec{z}_4$ is along the meson momentum direction in the laboratory frame ③.

two axes are chosen along its three momentum in different Lorentz frames, is called Wigner rotation, following his historical paper Ref. [23]. In this appendix, we give its simple derivation because it is not widely known to contemporary high energy physicists.

In Fig. 5, we show all the relevant Lorentz frames: The Lorentz frame ① and ④ is a vector boson rest frame, where angular-momentum-quantization axis $\vec{z}_1$ is chosen along the vector boson's three-momentum in the τ rest frame ②, while axis $\vec{z}_4$ is chosen along the vector boson's three-momentum in the laboratory frame ③. The τ rest frame ② is obtained from the laboratory frame ③ by a boost along the τ momentum direction $\vec{z}$ in the laboratory frame. Since the above successive transformations are all on the (z, x) plane, the quantization axis $\vec{z}_1$ in the vector boson rest frame is recovered by a rotation by $\tilde{\theta}$ about the common y-axis, namely, we have

$$1 = R_y(\tilde{\theta}) B_{z_4}^{-1}(y_{\rm v}) R_y(\theta) B_z(y_\tau) R_y(-\hat{\theta}) B_{z_1}(\hat{y}_{\rm v}), \quad \text{(A1)}$$

where $R_y(\theta) = e^{-iJ_2\theta}$ denotes rotation about the common y-axis and $B_z(y) = e^{-iK_3 y}$ denotes boost along the corresponding z-direction depicted in Fig. 5. Only two generators of the Lorentz transformations appear in Eq. (A1), whose nonzero components are $(J_2)_{jk} = -i\epsilon_{2jk}$, $(K_3)_{0k} = (K_3)_{k0} = i\delta_{k3}$. In Eq. (A1), $\hat{\theta}$ denotes the angle between z-axis and the vector boson three-momentum in the τ rest frame, θ denotes the angle between the z-axis and the vector boson's three-momentum in the laboratory frame, and $\tilde{\theta}$ is the Wigner rotation angle we want to derive. The rapidity along each direction satisfies

$$\tanh \hat{y}_{\rm v} = \hat{p}_{\rm v}/m_{\rm v} = \hat{k}, \quad \text{(A2a)}$$

$$\tanh y_\tau = p_\tau/m_\tau = \gamma\beta, \quad \text{(A2b)}$$

$$\tanh y_{\rm v} = p_{\rm v}/m_{\rm v} = \sqrt{\gamma^2(\beta\hat{\omega} + \hat{k}\cos\hat{\theta})^2 + (\hat{k}\sin\hat{\theta})^2}, \quad \text{(A2c)}$$

where $\hat{p}_{\rm v}$ denotes the vector boson's three-momentum in the τ rest frame, $p_{\rm v}$ denotes the vector boson's three-momentum in the laboratory frame, and p_τ denotes the τ lepton's three-momentum in the laboratory frame. Here, we have parametrized the τ lepton's four-momentum in the laboratory frame ③ as

$$p_\tau^\mu = (E_\tau, 0, 0, p_\tau) = m_\tau(\gamma, 0, 0, \gamma\beta). \quad \text{(A3)}$$

$\hat{p}_{\rm v}$ and the corresponding energy are easily derived as

$$\hat{E}_{\rm v} = \frac{m_\tau}{2}(1 + a^2) = m_{\rm v}\frac{1 + a^2}{2a} = m_{\rm v}\hat{\omega}, \quad \text{(A4a)}$$

$$\hat{p}_{\rm v} = \frac{m_\tau}{2}(1 - a^2) = m_{\rm v}\frac{1 - a^2}{2a} = m_{\rm v}\hat{k}, \quad \text{(A4b)}$$

with $a = m_{\rm v}/m_\tau$.

The vector boson's four-momentum in the laboratory frame can be expressed as

$$E_{\rm v} = m_{\rm v}\gamma(\hat{\omega} + \beta\hat{k}\cos\hat{\theta}), \quad \text{(A5a)}$$

$$p_{\rm v}^1 = m_{\rm v}\hat{k}\sin\hat{\theta}, \quad \text{(A5b)}$$

$$p_{\rm v}^2 = 0, \quad \text{(A5c)}$$

$$p_{\rm v}^3 = m_{\rm v}\gamma(\hat{k}\cos\hat{\theta} + \beta\hat{\omega}), \quad \text{(A5d)}$$

and hence $p_{\rm v}$ and $\tan\theta$ are derived as

$$p_{\rm v} = m_{\rm v}\sqrt{\gamma^2(\hat{k}\cos\hat{\theta} + \beta\hat{\omega})^2 + (\hat{k}\sin\hat{\theta})^2}, \quad \text{(A6)}$$

and

$$\tan\theta = \frac{\hat{k}\sin\hat{\theta}}{\gamma(\hat{k}\cos\hat{\theta} + \beta\hat{\omega})}. \quad \text{(A7)}$$

Equation (A6) determines the boost factor (A2c).

Straightforward calculation gives

$$R_y(\theta) B_z(y_\tau) R_y(-\hat{\theta}) B_{z_1}(\hat{y}) = \begin{pmatrix} \gamma(\hat{\omega} + \hat{c}\,\hat{k}\beta) & \gamma\hat{s}\beta & 0 & \gamma(\hat{k} + \hat{c}\,\hat{\omega}\,\beta) \\ \gamma s(\hat{c}\,\hat{k} + \hat{\omega}\beta) - c\hat{s}\,\hat{k} & c\hat{c} + \gamma s\hat{s} & 0 & \gamma s(\hat{c}\,\hat{\omega} + \hat{k}\beta) - c\hat{s}\,\hat{\omega} \\ 0 & 0 & 1 & 0 \\ \gamma c(\hat{c}\,\hat{k} + \hat{\omega}\beta) + s\hat{s}\,\hat{k} & -s\hat{c} + \gamma c\hat{s} & 0 & \gamma c(\hat{c}\,\hat{\omega} + \hat{k}\beta) + s\hat{s}\,\hat{\omega} \end{pmatrix}, \quad \text{(A8)}$$

where $c(\hat{c})$ and $s(\hat{s})$ denote $\cos\theta(\cos\hat{\theta})$ and $\sin\theta(\sin\hat{\theta})$, respectively. From the definition of the Wigner rotation Eq. (A1), we get that Eq. (A8) should be equal to the following quantity:

$$B_{z_4}(y_\mathrm{v})R_y(-\tilde{\theta}) = \begin{pmatrix} \cosh y_\mathrm{v} & \sinh y_\mathrm{v}\sin\tilde{\theta} & 0 & \sinh y_\mathrm{v}\cos\tilde{\theta} \\ 0 & \cos\tilde{\theta} & 0 & -\sin\tilde{\theta} \\ 0 & 0 & 1 & 0 \\ \sinh y_\mathrm{v} & \cosh y_\mathrm{v}\sin\tilde{\theta} & 0 & \cosh y_\mathrm{v}\cos\tilde{\theta} \end{pmatrix}. \tag{A9}$$

Comparison of (1,1) components of (A8) and (A9) gives

$$\cos\tilde{\theta} = \cos\theta\cos\hat{\theta} + \gamma\sin\theta\sin\hat{\theta}. \tag{A10}$$

In the Gallilean transformation limit with $\gamma = 1$, the Wigner rotation angle becomes

$$\tilde{\theta} = \hat{\theta} - \theta, \tag{A11}$$

as depicted in Fig. 5. In generic Lorentz transformations, the relation (A11) no longer holds, and the Wigner rotation angle $\tilde{\theta}$ is obtained from Eq. (A10). By inserting (A7) into (A10), we obtain

$$\cos\tilde{\theta} = \frac{\beta(1+a^2)\cos\hat{\theta} + 1 - a^2}{\sqrt{(\beta(1+a^2)+(1-a^2)\cos\hat{\theta})^2 + ((1-a^2)\sin\hat{\theta}/\gamma)^2}}, \tag{A12}$$

which gives Eq. (12) by noting $1/\gamma^2 = 1-\beta^2$.

Let us give a few remarks on the Wigner rotation angle $\tilde{\theta}$. As is clear from the expression Eq. (A6), the Gallilean limit of $\tilde{\theta} = \hat{\theta} - \theta$ is recovered for $\gamma \to 1$. Since $\gamma > 1$, the relativistic correction gives $\tilde{\theta} < \hat{\theta} - \theta$. In the ultrarelativistic limit with $\gamma \to \infty (\beta \to 1)$, we find

$$\cos\tilde{\theta} \underset{\beta\to 1}{\longrightarrow} \frac{(1+a^2)\cos\hat{\theta} + 1 - a^2}{(1-a^2)\cos\hat{\theta} + 1 + a^2}, \tag{A13}$$

which is a good approximation for a vector meson in the decay of a τ lepton coming from the decay of W, Z. Finally, it is worth noting that the expression Eq. (A9) gives the helicity conservation

$$\cos\tilde{\theta} \underset{a\to 0}{\longrightarrow} 1, \tag{A14}$$

in the massless limit of the vector meson with $a = m_\mathrm{v}/m_\tau \to 0$. There is no rotation ($\tilde{\theta} = 0$) in the massless limit, because the helicity of a massless particle is an invariant of Lorentz transformations.

[1] R. Aaij *et al.* (LHCb Collaboration), Observation of Photon Polarization in the $b \to s\gamma$ Transition, Phys. Rev. Lett. **112**, 161801 (2014).
[2] A. De Rùjula, R. Petronzio, and B. E. Lautrup, On the challenge of measuring the color charge of gluons, Nucl. Phys. **B146**, 50 (1978).
[3] H. Yang *et al.* (Belle Collaboration), Observation of $B^+ \to K_1(1270) + \gamma$, Phys. Rev. Lett. **94**, 111802 (2005).
[4] M. Gronau, Y. Grossman, D. Pirjol, and A. Ryd, Measuring the Photon Polarization in $B \to K\pi\pi\gamma$, Phys. Rev. Lett. **88**, 051802 (2002).
[5] M. Gronau and D. Pirjol, Photon polarization in radiative B decays, Phys. Rev. D **66**, 054008 (2002).
[6] E. Kou, A. Le Yaouanc, and A. Tayduganov, Determining the photon polarization of the $b \to s\gamma$ using the $B \to K_1(1270)\gamma \to (K\pi\pi)\gamma$ decay, Phys. Rev. D **83**, 094007 (2011).
[7] A. Tayduganov, E. Kou, and A. Le Yaouanc, Strong decays of K_1 resonances, Phys. Rev. D **85**, 074011 (2012).
[8] E. Kou, A. Le Yaouanc, and A. Tayduganov, Angular analysis of $B \to J/\psi K_1$: Towards a model independent determination of the photon polarization with $B \to K_1$ gamma, Phys. Lett. B **763**, 66 (2016).
[9] M. Gronau and D. Pirjol, Reexamining the photon polarization in $B \to K\pi\pi\gamma$, Phys. Rev. D **96**, 013002 (2017).
[10] D. G. Dumm, P. Roig, A. Pich, and J. Portoles, $\tau \to \pi\pi\pi\nu_\tau$ decays and the $a_1(1260)$ off-shell width revisited, Phys. Lett. B **685**, 158 (2010).
[11] O. Shekhovtsova, T. Przedzinski, P. Roig, and Z. Was, Resonance chiral Lagrangian currents and τ decay Monte Carlo, Phys. Rev. D **86**, 113008 (2012).
[12] I. M. Nugent, T. Przedzinski, P. Roig, O. Shekhovtsova, and Z. Was, Resonance chiral Lagrangian currents and experimental data for $\tau^- \to \pi^-\pi^-\pi^+\nu_\tau$, Phys. Rev. D **88**, 093012 (2013).
[13] J. H. Kühn and A. Santamaria, Tau decays to pions, Z. Phys. C **48**, 445 (1990).
[14] K. Ackerstaff *et al.* (OPAL Collaboration), A measurement of the hadronic decay current and the ν_τ helicity in $\tau^- \to \pi^-\pi^-\pi^+\nu_\tau$, Z. Phys. C **75**, 593 (1997).
[15] D. M. Asner *et al.* (CLEO Collaboration), Hadronic structure in the decay $\tau^- \to \nu_\tau\pi^-\pi^0\pi^0$ and the sign of the tau neutrino helicity, Phys. Rev. D **61**, 012002 (1999).
[16] B. K. Bullock, K. Hagiwara, and A. D. Martin, Tau polarization and its correlations as a probe of new physics, Nucl. Phys. **B395**, 499 (1993).

[17] R. Fischer, J. Wess, and F. Wagner, Decays of the heavy lepton τ and chiral dynamics, Z. Phys. C **3**, 313 (1980).
[18] J. Alwall, M. Herquet, F. Maltoni, O. Mattelaer, and T. Stelzer, MadGraph 5: Going beyond, J. High Energy Phys. 06 (2011) 128.
[19] K. Hagiwara, T. Li, K. Mawatari, and J. Nakamura, TauDecay: A library to simulate polarized tau decays via FeynRules and MadGraph5, Eur. Phys. J. C **73**, 2489 (2013).
[20] T. Sjostrand, S. Mrenna, and P. Z. Skands, A brief introduction to PYTHIA 8.1, Comput. Phys. Commun. **178**, 852 (2008).
[21] M. L. Mangano, M. Moretti, and R. Pittau, Multijet matrix elements and shower evolution in hadronic collisions: $Wb\bar{b}+n$ jets as a case study, Nucl. Phys. **B632**, 343 (2002).
[22] J. de Favereau, C. Delaere, P. Demin, A. Giammanco, V. Lemaître, A. Mertens, and M. Selvaggi (DELPHES 3 Collaboration), DELPHES 3, A modular framework for fast simulation of a generic collider experiment, J. High Energy Phys. 02 (2014) 057.
[23] E. P. Wigner, On unitary representations of the inhomogeneous Lorentz group, Ann. Math. **40**, 149 (1939); Nucl. Phys. B, Proc. Suppl. **6**, 9 (1989).